Hindawi Publishing Corporation
International Journal of Rotating Machinery
Volume 2014, Article ID 603241, 11 pages
http://dx.doi.org/10.1155/2014/603241

Research Article

A New Method for Field-Balancing of High-Speed Flexible Rotors without Trial Weights

Y. A. Khulief,[1] M. A. Mohiuddin,[2] and M. El-Gebeily[3]

[1] *Department of Mechanical Engineering, King Fahd University of Petroleum & Minerals, KFUPM Box 1767, Dhahran 31261, Saudi Arabia*
[2] *Data & Consulting Services, Schlumberger, Dhahran Tech Valley, Dhahran 31261, Saudi Arabia*
[3] *Department of Mathematics, King Fahd University of Petroleum & Minerals, KFUPM Box 1767, Dhahran 31261, Saudi Arabia*

Correspondence should be addressed to Y. A. Khulief; khulief@kfupm.edu.sa

Received 15 January 2014; Revised 20 April 2014; Accepted 21 May 2014; Published 15 June 2014

Academic Editor: Hyeong Joon Ahn

Flexible rotor balancing, in general, relies to a great extent on physical insight into the modal nature of the unbalance response. The objective of this investigation is to develop a hybrid experimental/analytical technique for balancing high-speed flexible rotors. The developed technique adopts an approach that combines the finite element modeling, experimental modal analysis, vibration measurements, and mathematical identification. The modal imbalances are identified and then transformed to the nodal space, in order to determine a set of physical balancing masses at some selected correction planes. The developed method does not rely on trial runs. In addition, the method does not require operating the supercritical rotor in a high-speed balancing facility, while accounting for the contribution of higher significant modes. The developed scheme is applied to a multidisk, multibearing, high-speed flexible rotor, where the interaction between the rotor-bending operating deflections and the forces resulting from the residual unbalance are appreciable. Some new benchmark solutions and observations are reported. The applicability, reliability, and challenges that may be encountered in field applications are addressed.

1. Introduction

Flexible rotors are of major concern to vibrations and balancing specialists, as they become increasingly integrated into many rotating machines. Generator rotors, in general, are flexible rotors; for example, power plant size generator rotors operate above the first and second bending modes, while long slender rotors run above the third or higher modes. Most turbine rotors are quasi-flexible, which imply that they operate above the first bending mode and sometimes the second. Flexible and quasi-flexible rotors exhibit appreciable dynamic response as they run through their critical speeds. According to ISO standards [1–3], flexible rotors are classified into five groups with different balancing techniques for each, wherein rigid body balancing could be applied to a group of flexible rotors when some special requirements are met; otherwise, high speed balancing must be used. Flexible rotor balancing is significantly more complex than rigid rotor balancing. The flexible rotor continually changes its elastic configuration as more critical speeds are encountered, and additional balance planes may be required. Since it is recognized that rotor-bending operating deflections modify the resulting forces from residual unbalance, flexible rotors need to be balanced at high speed.

Balancing flexible rotors has attracted the attention of many investigators during the last forty years. A number of pioneering investigations addressed some analytical and experimental aspects of the problem [4–6]. The *influence coefficient* and *modal balancing* techniques are the two principal approaches used for balancing flexible rotors. Modal balancing is not readily computerizable, as it relies on balancing the critical modes one by one and therefore requires high degree of operator insight. The number of correction planes used for modal balancing may also vary according to the adopted balancing scheme. The issue of the number of planes required for modal balancing of flexible rotors and whether it should

be n or n+ 2 planes (n is the number of critical speeds within the operating range) was debated at an early stage by Bishop and Parkinson [7] and Kellenberger [8]. However, practice has shown that rigid rotor balancing is a necessary step for a successful and efficient modal balancing.

Although the modal balancing has the advantage of minimizing the number of sensitivity runs at high speed, it relies on the assumption of planar modes. On the other hand, while the influence coefficient method suffers from the reliance on a significant number of sensitivity runs at high speed, it has the advantage of being adaptable to balancing any combination of critical speeds when full sensitivity information is available. Parkinson et al. [9] presented a theoretical study aimed at developing a unified approach to combine the advantages and alleviate the drawbacks of the two main approaches, namely, the influence coefficient and modal balancing techniques.

Some researchers attempted to perform modal balancing of flexible rotors without test runs in [10, 11]. Measurements of the vibration response were taken several times (four for each critical speed) and recorded close to the critical speeds as the rotor is being accelerated to the final service speed. In addition, they relied on a precalculated set of orthogonal test weights, [10]. Actually, it may not be practical to hold the rotor speed very close to its critical speed long enough to get good vibration readings. In general, their method requires the prior knowledge of mode shapes and generalized masses. Xu et al. [12] presented a genetic algorithm optimization procedure to formulate a rotor balancing method without test runs, which uses the balancing objective of influence coefficient method and the initial phase point of Holospectrum. The method was demonstrated experimentally on a two-disk flexible rotor running at speed above its first natural frequency. Yet, it was not tested at higher supercritical speeds. Sinha et al. [13] developed a procedure to estimate the misalignment and unbalance forces from a single run-down test, in conjunction with the FEM rotor model and the least-square method. They observed that the maximum error in the estimated unbalance amplitude was less than 45% for simultaneous random errors of 5% in the rotor model. It was suggested that the errors in the rotor model should be much less than 5% for many machines in practice.

Most of the previously cited methods were basically derived for isotropic rotors; yet, they are being used till now. Genta and Bona [14] presented a theoretical study that addressed the unbalance response calculation in the presence of damping, provided that a reliable model of the rotor damping is obtainable.

Flexible rotor balancing can be performed in the field at speeds well below 2000 rpm; otherwise, the rotor cannot be run with open casing due to safety hazards. In this case, field balancing will be costly and time consuming due to opening the rotor casing for correction or trial weight application and then closing the rotor before each run. In addition, there are significant risks and costs associated with balancing a rotating element in the field. Every time a casing is opened, there is a chance to introduce foreign objects into the flow path or to damage a component. In general, it is often necessary to balance the rotor at full operating speed after overspeed testing. Such full-speed balancing needs to be performed in high-speed balancing facility.

Regardless of the method invoked for flexible rotor balance, turbomachinery users remained concerned about the increased cost and possible downtime associated with field balancing of high-speed rotors due to its limitations and difficulties. On the other hand, using high-speed balancing facility is costly and may require the rotor to be shipped to a distant location, which poses logistical inconvenience and increased downtime. Zlatan [15] presented a case of high-speed balancing of generator rotor, in which it was concluded that the rotor had undergone runout changes as a result of dynamic bending conditions during balancing, and, therefore, the rotor exhibited unusual behavior when installed in the field. Accordingly, the expensive and complicated high-speed balancing may not arrive at satisfactory results in all cases.

Very few investigations were reported, which addressed the development of low-speed techniques for balancing high-speed rotors. Tan and Wang [16] presented an analytical approach unifying the modal balancing and the influence coefficient methods. The unified theory was applied to the low-speed balancing of flexible rotors. It was then suggested that under certain requirements, a rotor could be balanced at low-speeds (influence-coefficient method), whilst meeting the requirements of high speed (modal) balancing. No experimental verifications were reported, however. Shi [17] presented a Low-Speed Holo-Balancing (LSHB), which can balance the flexible rotor without test runs at high speeds. The principle of LSHB is mainly based on the holospectrum technique, in which the vibration response of rotor is described by three-dimensional holospectrum using multisensor fusion. The method, however, relies on gaining insight into the variation of the modal components through the information in run-up or run-down stages.

In the previous investigations, a reliable rotor dynamic model was always placed at the core of most of the developed methods of flexible rotor balancing. In this context, researchers continued to develop some revised balancing schemes by utilizing the FEM modeling of the rotor. Kang et al. [18] employed the FEM model of the rotor into a balancing scheme, in which they optimized the imbalance estimates by minimizing the condition number of the influence coefficients. They used trial masses, while the rotor was run at speeds above its critical speeds during the balancing sessions. The model-based methods for fault identification were adapted by some investigators to estimate the flexible rotor unbalance [19]. The experimental results were found to agree well with the simulated results. It was also concluded that the equivalent loads minimization method with modified theoretical fault model and vibration minimization method are more effective than the equivalent loads minimization method alone in identifying unbalance fault with reasonably less error. Li et al. [20] utilized the finite element method to obtain the rotor's modal characteristics. They represented the rotor response in terms of a modal expansion and calculated the correction masses based on vibration measurements close to the critical speed without trial weights.

The aforementioned literature review reveals that regardless of the method used, the existing techniques for balancing flexible rotors rely on conducting balancing sessions at balancing speeds equal or close to the rotor critical speeds, within the operating range. Accordingly, such techniques often need to be performed in a high-speed balancing facility. Most of the available methods use several test runs with trial masses. In addition, the majority of the modal balancing techniques adopt mode-by-mode balancing, thus ignoring spillover from other higher modes. In general, such techniques require high degree of operator insight, because there is no systematic method for balancing flexible rotors. In this paper, a method for balancing flexible rotors, which overcomes some of the stated difficulties, is developed. The developed technique adopts an approach that combines the finite element modeling, experimental modal analysis, vibration measurements, and mathematical identification. The method is equally applicable to isotropic as well as anisotropic flexible rotors. The experimental measurements of the rotor unbalance response are done either directly or via the measured operational deflection shapes obtained by operational modal analysis (OMA) at service speed. The method does not rely on trial runs and can be adopted for field balancing of supercritical rotors, while accounting for the modal contribution of several significant modes.

2. The Balancing Formulation

The elastodynamic model of the rotor system is formulated using the finite element method. In this regard, an accurate finite element model of the rotor is a prerequisite for the accuracy of the developed balancing scheme. Let the rotor equation of motion be written in the form

$$\mathbf{M}\ddot{\mathbf{q}} + \mathbf{C}\dot{\mathbf{q}} + \mathbf{K}\mathbf{q} = \mathbf{F}, \tag{1}$$

where $\mathbf{M} \in \mathbb{R}^{n\times n}$ is the mass matrix, $\mathbf{C} \in \mathbb{R}^{n\times n}$ is the matrix that absorbs both damping and gyroscopic effects, $\mathbf{K} \in \mathbb{R}^{n\times n}$ is the stiffness matrix, $\mathbf{q} \in \mathbb{R}^n$ is the vector of physical coordinates, which may represent nodal coordinates in the finite element discretization, and $\mathbf{F} \in \mathbb{R}^n$ is the forcing vector. Details of the finite element dynamic modeling of multidisk multibearing rotor systems are presented in [21–23]. In addition, the rotordynamics module of the commercial software ANSYS can be utilized for modeling the intricate details of complex rotor systems, while accounting for the rotational effects.

In system identification, the displacement vector $\mathbf{q}$ is obtained by measurements of the system's response, either directly using displacement transducers or indirectly using accelerometers. Assume the dominant frequency subspace spans a set of m significant modes $\mathbf{\Phi} \in \mathbb{R}^{n\times m}$. Normally, the set of significant modes includes lower modes of vibration that contain most of the system's kinetic energy within the band of the excited frequencies. In this investigation, the significant mode shapes or eigenvectors are determined experimentally using either experimental modal analysis (EMA) or operational modal analysis (OMA), as explained later. Now, (1) can be written in the reduced-order modal space as

$$\mathbf{M}_m\ddot{\mathbf{u}} + \mathbf{C}_m\dot{\mathbf{u}} + \mathbf{K}_m\mathbf{u} = \mathbf{Q}_m, \tag{2}$$

where $\mathbf{u} = \mathbf{\Phi}^T\mathbf{q} \in \mathbb{R}^m$, vector of the distributed modal coordinates, $\mathbf{M}_m = \mathbf{\Phi}^T\mathbf{M}\,\mathbf{\Phi} \in \mathbb{R}^{m\times m}$, modal mass matrix, $\mathbf{C}_m = \mathbf{\Phi}^T\mathbf{C}\mathbf{\Phi} \in \mathbb{R}^{m\times m}$, modal damping matrix, $\mathbf{K}_m = \mathbf{\Phi}^T\mathbf{K}\mathbf{\Phi} \in \mathbb{R}^{m\times m}$, modal stiffness matrix, and $\mathbf{Q}_m = \mathbf{\Phi}^T\mathbf{F} \in \mathbb{R}^m$, modal forcing vector.

It is important to note that, at steady operational conditions, the excitation $\mathbf{F}$ is due only to harmonic imbalance excitations. Employing the Fourier transform, one can write (2) in the frequency domain as

$$\left[-\omega^2\mathbf{M}_m + j\omega\mathbf{C}_m + \mathbf{K}_m\right]\mathbf{U}(\omega) = \mathbf{Q}_m(\omega), \tag{3}$$

where $\mathbf{U}(\omega) \in \mathbb{C}^m$ and $\mathbf{Q}_m(\omega) \in \mathbb{C}^m$ are the Fourier transforms of their time counterparts. Equation (3) can be rewritten as

$$\left[-\omega^2\mathbf{I}_m \quad j\omega\mathbf{I}_m \quad \mathbf{I}_m\right]\begin{bmatrix}\mathbf{M}_m\\ \mathbf{C}_m\\ \mathbf{K}_m\end{bmatrix}\mathbf{U}(\omega) = \mathbf{Q}_m(\omega), \tag{4}$$

where $\mathbf{U}(\omega)$ is known from measurements and $\mathbf{I}_m$ is the $m\times m$ identity matrix. Let us define the operator $\mathrm{vec}(\cdot): \mathbb{R}^{m\times n} \to \mathbb{R}^{mn}$ by

$$\mathrm{vec}(\mathbf{A}) = \left[\mathbf{A}_1^T \quad \mathbf{A}_2^T \quad \cdots \quad \mathbf{A}_n^T\right]^T, \tag{5}$$

where $\mathbf{A}_1, \mathbf{A}_2, \ldots, \mathbf{A}_n$ are the columns of the matrix $\mathbf{A}$. There is a usual relationship between the vec$(\cdot)$ operator and the Kronecker product [24], which is given as

$$\mathrm{vec}(\mathbf{AXB}) = \left(\mathbf{B}^T \otimes \mathbf{A}\right)\mathrm{vec}(\mathbf{X}), \tag{6}$$

where $(\mathbf{B}^T \otimes \mathbf{A})$ is the Kronecker product of the matrices $\mathbf{B}^T$ and $\mathbf{A}$. Using this relation, one can rewrite (4) in the form

$$\mathbf{U}^T(\omega) \otimes \left[-\omega^2\mathbf{I}_m \quad j\omega\mathbf{I}_m \quad \mathbf{I}_m\right]\mathrm{vec}\left(\begin{bmatrix}\mathbf{M}_m\\ \mathbf{C}_m\\ \mathbf{K}_m\end{bmatrix}\right) = \mathrm{vec}\left(\mathbf{Q}_m(\omega)\right), \tag{7}$$

which is a linear system of the form $\mathbf{Ax} = \mathbf{b}$. For a set of frequencies ω_i, $i = 1, 2, \ldots$. Equation (7) gives rise to

$$\mathbf{A} = \begin{bmatrix}\mathbf{U}(\omega_1) \otimes \left[-\omega_1^2\mathbf{I}_m \quad j\omega_1\mathbf{I}_m \quad \mathbf{I}_m\right]\\ \mathbf{U}(\omega_2) \otimes \left[-\omega_2^2\mathbf{I}_m \quad j\omega_2\mathbf{I}_m \quad \mathbf{I}_m\right]\\ \vdots\\ \mathbf{U}(\omega_r) \otimes \left[-\omega_r^2\mathbf{I}_m \quad j\omega_r\mathbf{I}_m \quad \mathbf{I}_m\right]\end{bmatrix} \in \mathbb{C}^{rm\times 3m^2},$$

$$\mathbf{x} = \mathrm{vec}\left(\begin{bmatrix}\mathbf{M}_m\\ \mathbf{C}_m\\ \mathbf{K}_m\end{bmatrix}\right) \in \mathbb{R}^{3m^2}, \tag{8}$$

$$\mathbf{b} = \begin{Bmatrix}\mathbf{Q}_m(\omega_1)\\ \mathbf{Q}_m(\omega_2)\\ \vdots\\ \mathbf{Q}_m(\omega_r)\end{Bmatrix} \in \mathbb{C}^{rm}.$$

Here, the entries of the coefficient matrix $\mathbf{A}$ are obtained from measurements of the system response $\mathbf{U}(\omega)$ at the set of frequencies ω_i, $i = 1, 2, \ldots, r$. The vector $\mathbf{x}$ is also known, as its components are determined from the finite element model together with the experimental modal analysis. In this context, the modal mass, stiffness, and damping matrices are obtained from the corresponding finite element matrices by a modal transformation comprising a set of experimentally measured mode shapes. The only unknown in (7) is the right side $\mathbf{Q}_m(\omega)$, which represents the excitation forces. It is worth mentioning that (7) can also be utilized for identification of the system parameters $\mathbf{M}_m$, $\mathbf{C}_m$, and $\mathbf{K}_m$, based on the obtained measurements of the input excitation $\mathbf{b}(\omega)$ and response $\mathbf{U}(\omega)$ [25].

Accordingly, the developed balancing scheme is essentially an inverse dynamics approach, wherein the harmonic excitation provoked by the unbalance is being the target of the identification process. This is the crux of the developed balancing scheme. Normally, a rotor system, away from startup and shutdown, is run at a constant service speed. In such a mode of steady operating conditions, the primary excitation in the radial direction is due to centrifugal forces resulting from the residual unbalance. It is also known that the harmonic excitation force resulting from unbalance is simply a centrifugal force $f_i(\omega_j)$, which is a function of the rotational speed. The unbalance excitation appears as a peak on the frequency spectrum at the matching frequency to the rotational speed, which is commonly used as a basis for order analysis in diagnostics of rotating machinery. Such a centrifugal force can be written as $f_i(\omega_j) = \alpha_i \omega_j^2$, where $\alpha_i \in \mathbb{C}^2$ is the imbalance existing at the ith measurement plane.

Now, let us present the balancing procedure based on the developed inverse scheme. The previous calculations (see (7)) produce the modal imbalances $\mathbf{Q}_m(\omega)$, which upon transformation back to nodal space will result in the physical imbalances at some selected planes. Recall that, at steady operation, the modal imbalances can be written in terms of a set of nodal imbalances $\mathbf{Q} \in \mathbb{R}^n$ as

$$\mathbf{Q}_m = \mathbf{\Phi}^T \mathbf{Q} \in \mathbb{R}^m. \tag{9}$$

To solve this underdetermined system for $\mathbf{Q}$, let us assume that $\mathbf{\Phi}^T$ has full rank m. This condition is directly satisfied for linear modal transformations. wherein the basis of the modal space is composed of a set of significant (independent) modes. Accordingly, one can select m linearly independent columns out of the n columns of $\mathbf{\Phi}^T$. Suppose we arrange these$m$ columns in a matrix $\mathbf{D}$. Then one can rearrange the columns of the matrix $\mathbf{\Phi}^T$ in such a way that the columns of the matrix $\mathbf{D}$ become the first m columns of the rearranged matrix. The rearranged matrix will then have the partitioned form $[D : E]$, where E is the $m \times (n - m)$ matrix consisting of the remaining columns of $\mathbf{\Phi}^T$. This rearrangement of the columns can, as a matter of fact, be effected by multiplying $\mathbf{\Phi}^T$ on the right by an $n \times n$ matrix $\mathbf{H}$, which is a permutation of the columns of the $n \times n$ identity matrix. Performing this multiplication gives the following:

$$\mathbf{\Phi}^T \mathbf{H} = [\mathbf{D} : \mathbf{E}]. \tag{10}$$

With the numerical stability and accuracy properties in mind, it is suggested that the submatrix $\mathbf{D}$ should be chosen with the minimum possible condition number. Therefore, we have the following decomposition:

$$\begin{aligned} \mathbf{D}^{-1}\mathbf{Q}_m &= \mathbf{D}^{-1}\mathbf{\Phi}^T\mathbf{Q} \\ &= \mathbf{D}^{-1}\mathbf{\Phi}^T\mathbf{H}\mathbf{H}^{-1}\mathbf{Q} \\ &= \mathbf{D}^{-1}\left[\mathbf{D} : \mathbf{E}\right]\mathbf{H}^{-1}\mathbf{Q} \\ &= \left[\mathbf{I}_m : \mathbf{D}^{-1}\mathbf{E}\right]\mathbf{H}^{-1}\mathbf{Q} \\ &= \left[\mathbf{I}_m : \widetilde{\mathbf{E}}\right]\widetilde{\mathbf{Q}} \end{aligned} \tag{11}$$

with $\widetilde{\mathbf{E}}$ and $\widetilde{\mathbf{Q}}$ obviously defined. Observe that $\widetilde{\mathbf{Q}}$ is just a rearrangement of the elements of $\mathbf{Q}$. In other words, its elements still correspond to nodal imbalances. Decomposing $\widetilde{\mathbf{Q}}$ as

$$\widetilde{\mathbf{Q}} = \begin{bmatrix} \widetilde{\mathbf{Q}}_1 \\ \widetilde{\mathbf{Q}}_2 \end{bmatrix}, \tag{12}$$

where $\widetilde{\mathbf{Q}}_1$ and $\widetilde{\mathbf{Q}}_2$ are $m \times 1$ and $(n-m) \times 1$ vectors, respectively. We may rewrite (11) as

$$\widetilde{\mathbf{Q}}_1 = \mathbf{D}^{-1}\mathbf{Q}_m - \widetilde{\mathbf{E}}\widetilde{\mathbf{Q}}_2. \tag{13}$$

Equation (13) gives the nodal imbalance assignments for any arbitrary choice of the free variables $\widetilde{\mathbf{Q}}_2$. One can, for example, assign to any $r-m$ components of $\widetilde{\mathbf{Q}}_2$ nonzero values ($n \geq r \geq m$) and set the remaining $n - r$ components to zero, compute the corresponding nodal imbalances $\widetilde{\mathbf{Q}}_1$ from (13), and then recover $\mathbf{Q} = \mathbf{H}\,\widetilde{\mathbf{Q}}$. Generally, in this case, $\mathbf{Q}$ has r nonzero components, $n \geq r \geq m$. The most popular choice is $r = n$, which corresponds to choosing $\widetilde{\mathbf{Q}}_2 = 0$. It is also noted that the choice $\widetilde{\mathbf{Q}}_2 = (\widetilde{\mathbf{E}}^T\widetilde{\mathbf{E}})^\dagger \widetilde{\mathbf{E}}^T \mathbf{D}^{-1}\mathbf{Q}_m$, where $(\cdot)^\dagger$ stands for the Moore-Penrose inverse, corresponds to $\widetilde{\mathbf{Q}}_1$ with the minimum norm.

3. Balancing Procedure

(1) Construct a finite element model of the rotor-bearing system that accounts for all structural details and dynamic effects.

(2) Carry out experimental modal analysis (EMA) on the rotor system and determine the significant set of m mode shapes. Typically, for modal transformation, we can choose any reasonable number of modes to construct modal matrices, that is, a few modes above the operating speed. For example, if the rotor rotates above the 2nd natural frequency, then we may consider the first three to five modes as significant. It

is important to note that the obtained experimental mode shapes depend on the structural properties of the rotor and therefore account for the residual mass unbalance effects. Normalize the mode shapes and construct the modal matrix $\mathbf{\Phi} \in \mathbb{R}^{n\times m}$, [26].

(3) Carry out modal transformations using the experimentally identified mode shapes as a basis for the transformation and obtain the modal matrices $\mathbf{M}_m$, $\mathbf{C}_m$, and $\mathbf{K}_m$.

(4) Measure the system response $\mathbf{E}(\omega)$ of the rotor at a set of selected rotational speeds ω_i, $i = 1, 2, \ldots, r$. In fact, measurements are only needed at the rotor's operating speed. It is also possible to obtain measurements at a few other speeds in the operating range to verify the robustness of measurements. This step is carried out *in situ*, and can be done directly if the required measurements locations are accessible. Alternatively, the system response can be obtained using Operational Modal Analysis (OMA) of the rotor at the selected operating speed, plotting Operational Deflection Shapes (ODS) and measuring the response at the measurement planes.

(5) Solve (7) to calculate the right side, which represents a set of existing modal imbalances.

(6) Transforming back to nodal space will result in the physical imbalances at some selected correction planes, as given by (13).

It is noted that the vector $\widetilde{\mathbf{Q}}$ has entries corresponding to the two transverse nodal coordinates, which are consistent with the retained bending modes of the modal transformation. That is, the vector $\widetilde{\mathbf{Q}}$ contains pairs of x and y components of the nodal imbalances within the nodal planes. However, selecting a set of correction planes is achieved by $\widetilde{\mathbf{Q}}_1$ in (13). Observing that $\widetilde{\mathbf{Q}}_1$ has the same dimension m as the basis of the modal transformation, one can set a criterion for the number of correction planes in relation to the number of critical speeds within the operating range. If the rotor is supercritical to the kth degree (k represents the number of modes within the operating range), then the *number* of modal imbalances $\mathbf{Q}_m$ in (13) is given by

$$m = 2(k + 1) \tag{14}$$

and the number of the correction planes is given by $m/2$. For instance, if the rotor's operating speed is higher than the 2nd mode, then we use $m = 2(2 + 1) = 6$ modal imbalances and apply corrections in 3 planes. One of the robust features of this method is that the contribution of several significant modes, above the highest critical speed, are taken into account in the calculation of the correction masses. This will account for mode coupling due to damping and the possible higher frequency excitations. As seen in this example, six modal imbalances were used in the transformation for the case when the rotor runs above the second critical speed.

In essence, the developed method is an $N + 1$ plane balancing, where N is the number of critical speeds in the operating range. It is worth mentioning that the flexible rotor is presumed to have a small amount of residual unbalance when run as a rigid rotor (i.e., below the first critical). Unlike some pervious methods [10], which rely on a known value of the constrained shaft bow to serve as a source of harmonic excitation at high speed, our method relies on the residual unbalance which exists naturally in any rotor. This requirement is mandated by the FEM generation of the mass and stiffness matrices, which are calculated for an unbalance-free rotor. That is, in some situations, one may need to start with rigid rotor balancing, if the rotor manifests an appreciable unbalance at low speed, as a prerequisite for flexible balancing. In fact, getting rid of the excessive unbalance at low speed is also mandated by the rotor's operability. We found experimentally that a rotor, which is unbalanced as rigid, may experience excessive deflections if brought to supercritical speeds, thus forcing a rundown to avoid damage to the bearings.

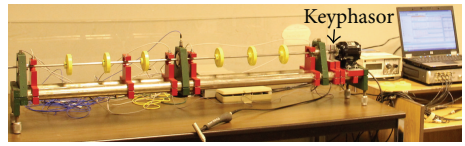

Figure 1: The instrumented 6-disk rotor-bearing system.

4. Experimental Setup

An experimental rotor-bearing test rig was designed and manufactured to carry out the experimental verification of the developed balancing method. The rotor system consists of 120 cm stainless steel shaft, mounted on three rolling element bearings with rubber-padded housings to increase external damping, as shown in Figure 1, which includes six identical steel disks. The shaft diameter is 10 mm, the disk outer diameter is 76.2 mm, and disk thickness is 12.7 mm. The rotor surface under the probe tip was machined at surface roughness grade N1 to minimize the possibility of the dc gap effect. The rotor system is driven by a speed-controlled DC motor, which runs at a maximum 10,000 rpm. The rotor system was designed to have its first three critical speeds well below the maximum motor speed. Table 1 shows the first five undamped natural frequencies of the rotor-bearing system. Figure 2 shows the first two modes shapes as predicted by the finite element model. For comparison between the FEM prediction and the experimentally identified modes, the normalized planar projections of the first two modes are presented in Figure 3. The rotor was instrumented with eight proximity probes, at both vertical and horizontal directions, in addition to three accelerometers at the bearings and one proximity probe as a phase indicator. Both accelerometers and proximity probes as marked in Figure 4 and numbered from the motor side (inboard rotor side). The measurements from all transducers are acquired, conditioned, and processed by LMS Pimento 12-channel data acquisition and analysis system. The LMS hardware is driven by a bundle of analysis software including order analysis, experimental modal analysis, and operational modal analysis. The LMS

Table 1: Natural frequencies of the rotor.

Mode number	Natural frequencies (Hz)		Measured modal damping (%)
	Calculated (FEM)	Measured (EMA)	
1	20.563	20.358	0.302
2	64.428	63.917	0.285
3	123.682	122.153	0.254
4	183.213	180.636	0.228
5	265.147	262.523	0.206

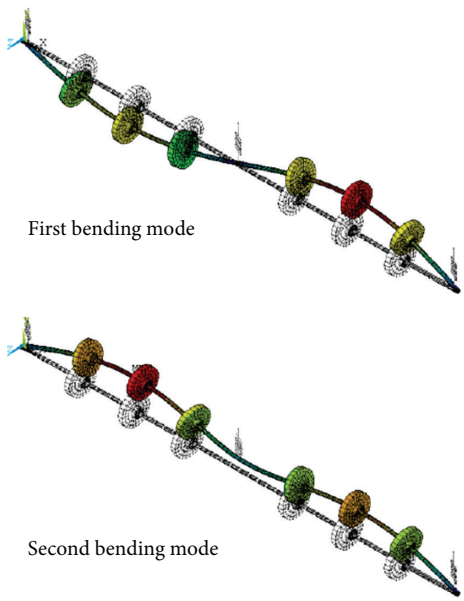

Figure 2: Modes shapes obtained by FEM.

system is used for measurements and modal processing at a frequency bandwidth of 3200 Hz, which is linked to the sampling rate through Shannon's theorem (i.e., sampling rate is 6400 Hz). The block size is 16384 which defines the frequency resolution.

5. Experiential Runs

After proper alignment is performed, the runout *P-P* value was measured, which was found to be very small; in the range of 0.34 mils (i.e., in the order of (1/20)th the dynamic response amplitude, which is negligible according to API standards). First, the rotor was accelerated slowly up to 700 rpm (below the first critical) and the slow roll was observed to be small, as shown in the filtered uncompensated amplitude and phase graphs of Figure 5 for the mid-span Probe 3 as numbered from the motor side. Second, the two-plane balancing of rigid rotors was conducted at 900 rpm, which resulted in a balanced rotor at this speed with the bearing signature indicating an amount of residual unbalance, as shown in Figure 6 that represents the vertical accelerometer output mounted on the second bearing V2. It is important to note that our main emphasis in the test runs is to demonstrate the applicability of the developed balancing scheme. As for balancing quality grade, we considered that this shaft configuration to lie within the wide range of quality grade G6.3, and we considered an acceptance level to be below 5 mm/s. In addition, the percentage unbalance reduction is considered a realistic measure of the success of the balancing process and will be adopted in this investigation for verification purposes. In practice, the international standards [2, 3] and ISO 1940-1 [27] are frequently used to determine balancing quality and balancing procedure for flexible rotors. The nearest American equivalents are the standard ANSI S2.42 and ANSI S2.43 as presented by the latest revisions [28, 29], respectively.

Before starting the experimental procedure of the new balancing scheme, which is mainly dependent on the fidelity of the experimental modal data, an extensive uncertainty analysis of the modal data was performed. For brevity and without diverting from the emphasis of the paper, we considered both random (force level, input location, and algorithmic) and bias (support conditions, mass loading, instrumentation cable defects, and ambient environment) sources. Uncertainty due to input location and force level were evaluated simply by performing a few additional tests at different locations, in addition to repeated measurements at a single location with varying levels. For each individual test, the input level for all averages was maintained within 10% margin below or above the nominal value, while rejecting values outside this margin. Because such tests were performed in a controlled lab environment, the ambient conditions uncertainty is assumed insignificant for these tests. This uncertainty was evaluated by the Synthesis Modes and Correlate Algorithm (SMAC). For instance, we repeated measurements at a few different excitation locations to evaluate this inherent uncertainty. By analyzing the selected frequency range of 10–300 Hz, we found that the inherent uncertainty in frequency is 0.06% and for modal damping is 1.87%. For some modes, the inherent frequency uncertainty is less than 0.003%; however, we chose the conservative value. Other details of the uncertainty analyses are presented in [30].

In the next part of the investigation, the developed balancing scheme is applied to the experimental rotor under the two following operating conditions.

(a) First, the rotor is run at 2700 rpm, which is above the first critical speed. Figure 7 shows that the flexible rotor is experiencing an appreciable amount of unbalance, when run at this high speed. One of the interesting observations is that a relatively small residual unbalance at subcritical speeds may develop into a much larger amount of unbalance at supercritical speeds. Noting that disks are numbered 1 to 6 from the motor side, the correction planes are labeled accordingly; that is, correction plane i is simply disk i, as shown in Figure 4. A correction radius of 3.175 cm is used in all planes. The balancing procedure is carried out as stated in Section 3, in which the influence of the first four modal contributions are considered in the calculations, according to the rule stated by (14). In this case, two correction planes are required, that is, disks 2 and 5. The calculated correction masses are $M_2 = 24.6\,\text{gm}$ at $\angle 76.3^\circ$ and $M_5 = 19.2\,\text{gm}$ at $\angle 169.6^\circ$. The first critical speed of this rotor, by its very nature, leads one to directly select planes 2 and 5, where the modal

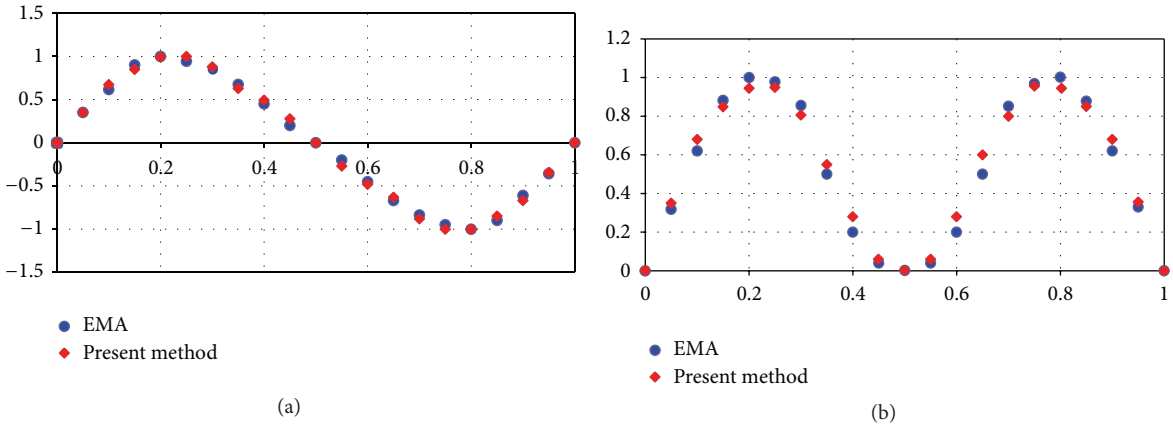

Figure 3: (a) The First mode shape and (b) the second mode shape.

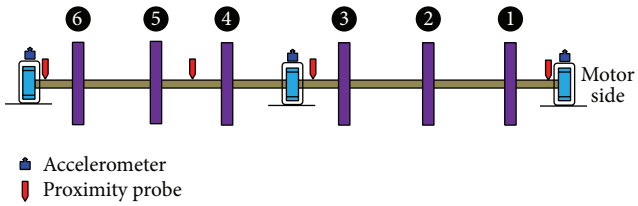

Figure 4: The numbering of balancing planes.

Table 2: The correction masses.

Correction planes* (Set 1)			Correction planes* (Set 2)		
Number	Mass (gm)	Angle (deg)	Number	Mass (gm)	Angle (deg)
S_1	12.766	31.532	S_1	14.221	157.812
S_2	21.521	173. 153	S_2	11.783	96.214
S_5	17.926	−148.538	S_4	19.343	67.229
S_6	9.833	−63.645	S_5	13.327	−87.556

*Correction planes are numbered from the motor side.

amplitude is the largest. The balanced rotor response is shown in Figure 8, with an unbalance reduction of nearly 70%. As a result of the redundancy expressed by the availability of more than one choice of the matrix D in (10), carrying out calculation for planes 1 and 6 or 1 and 4 would do the job as well; yet the correction masses may assume a little higher value. For instance, the calculated correction masses for planes 1 and 6 are $M_1 = 29.6$ gm at $\angle 94.2^\circ$ and $M_6 = 32.7$ gm at $\angle 208.4^\circ$, and the resulting residual unbalance was very close to that of Figure 8. In this context, we may refer to one nice feature of this scheme, which is manifested by the simplicity of testing different sets of correction planes by merely solving the linear system resulting from (7), once measurements and experimental modal analysis data are recorded.

(b) In the second experimental test, the clean rotor is operated at 9000 rpm, which exceeds its third critical speed. The vibration spectrum is shown in Figure 9, where, in addition to the eruption of sever unbalance, some excitations at the critical frequencies are visible. The developed balancing scheme is invoked to balance the rotor. In this case, according to the rule of (14), eight modal imbalances will be involved in calculating the correction masses to be added in a selected set of four planes. In this regard, two sets of correction planes are selected to demonstrate the influence of locations of the correction planes on the degree of sensitivity to the rotor's modal deformations. The two sets of correction planes and the corresponding calculated sets of correction masses are listed in Table 2. Figures 10 and 11 show the rotor's response after balancing. The degree of unbalance reduction was different for the two sets of correction planes. While the first set of correction planes resulted in about 62% unbalance reduction, the second set showed better results at 78% unbalance reduction. For this nicely behaving experimental rotor, it is apparent that having a correction plane closer to the middle bearing would have better mode observability, as manifested by the second set which includes plane 4. In actual large-scale rotors, the experimentally identified mode shapes will serve as a guide for judging the proper set of correction planes. This does not mean, of course, that visual inspection of mode shapes would definitely lead to the selection of the best set of correction planes. Modal coupling in actual rotors with some appreciable damping may require testing some alternative planes, as well. There is no need to postulate the existence of optimal locations of the correction planes at this stage, as the unbalance reduction is our target. However, this may be posed as a problem for further research.

Two interesting observation were gleaned out from this later case. After balancing the rotor beyond its third critical speed, we run the rotor above its first critical (at speed of 2700 rpm). As shown in Figure 12, the rotor remained balanced, however the residual unbalance increased slightly over the previous balancing session of Figure 8, in which the balancing procedure was intended to target the first frequency. Such increase in unbalance may be attributed to modal coupling effects. A second run is made for the same balanced rotor at a speed of 900 rpm, that is, below its first critical or simply as a rigid rotor. It was noted that

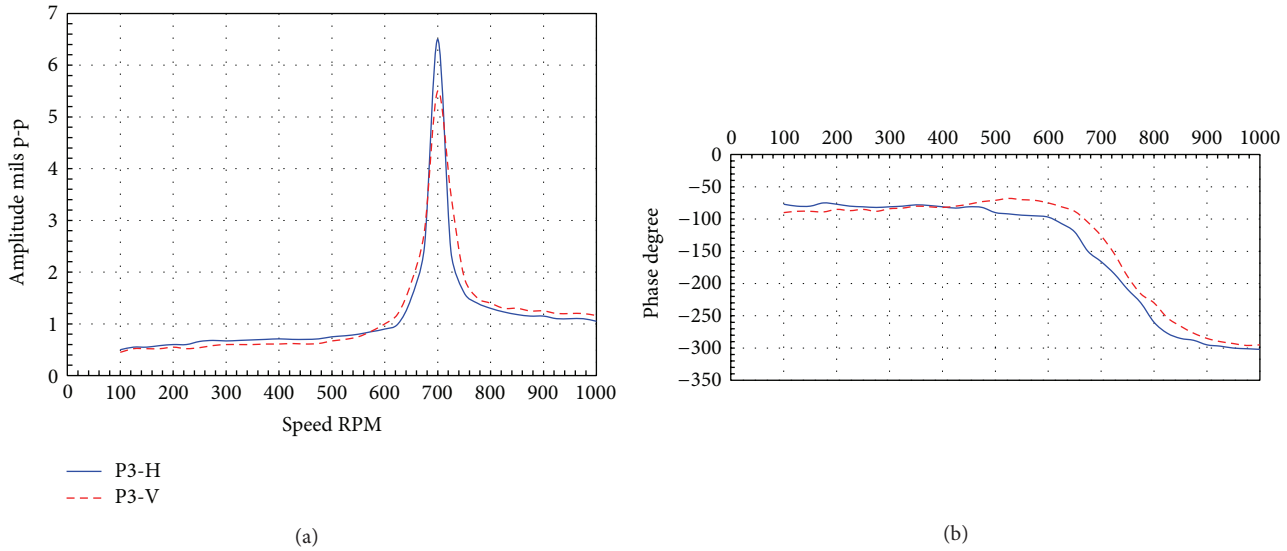

FIGURE 5: The slow roll data at location-3: P3-H: horizontal; P3-V: vertical.

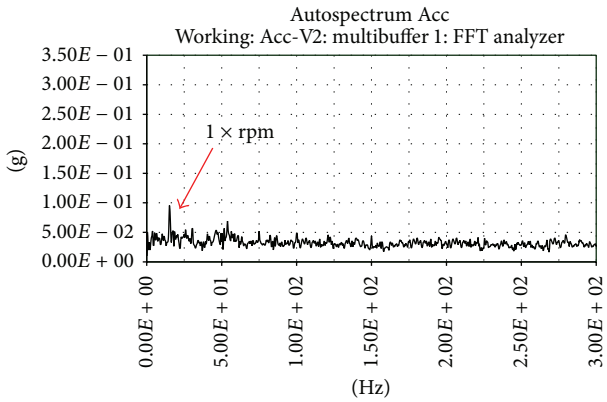

FIGURE 6: The residual unbalance (rotor running subcritical at 900 rpm).

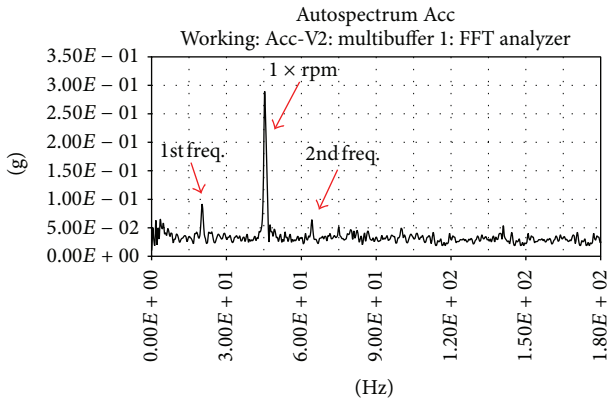

FIGURE 7: The rotor running supercritical at 2700 rpm, before balancing.

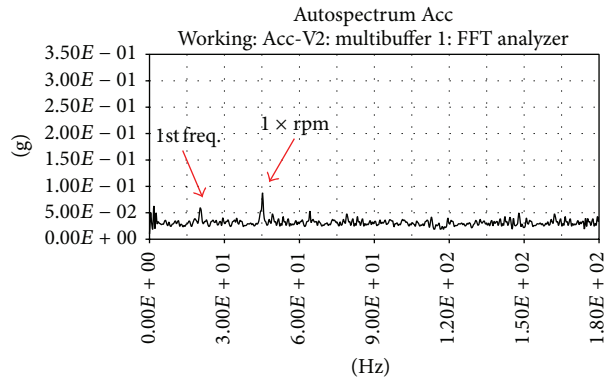

FIGURE 8: The rotor running supercritical at 2700 rpm, after balancing.

the rigid rotor initial residual unbalance has appreciably increased, as shown in Figure 13. It comes as no surprise that with the modal balancing primarily directed to imbalance-deformation interaction, the resulting corrections are likely to be insensitive to the rigid rotor imbalance. This observation alarms the user to check the low speed residual unbalance after the high-speed balancing session is concluded to decide whether a trim balancing session is required. However, if this value is far below the operating speed, then the operator may just cross it quickly during the startup protocol.

6. Conclusions

A balancing scheme for high-speed flexible rotors is developed. The method is well-suited for field balancing without trial runs. One of the unique features of the method is the accountability of the effect of several modes, including few modes above the highest critical speed, in calculating the

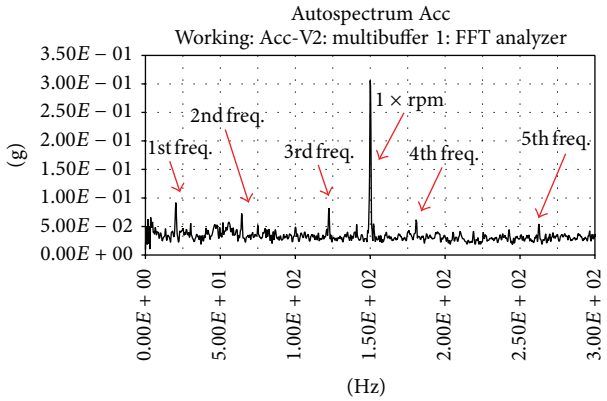

Figure 9: The rotor running supercritical at 9000 rpm, before balancing.

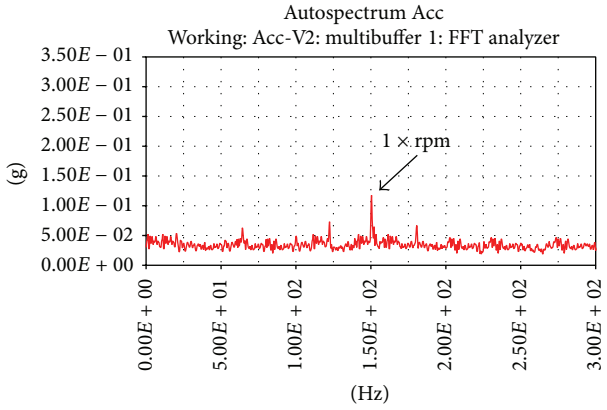

Figure 10: The rotor running supercritical at 9000 rpm (after balancing at 1st set of correction planes).

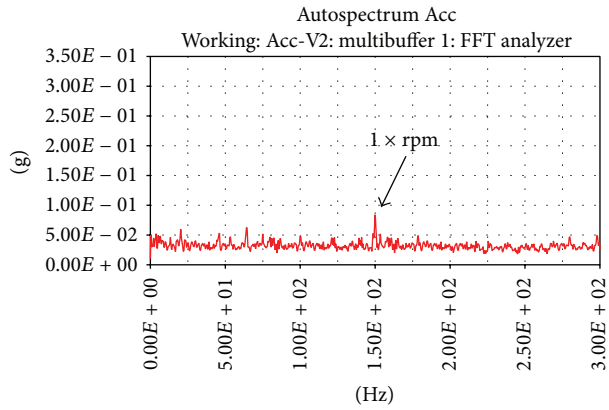

Figure 11: The rotor running supercritical at 9000 rpm (after balancing at 2nd set of correction planes).

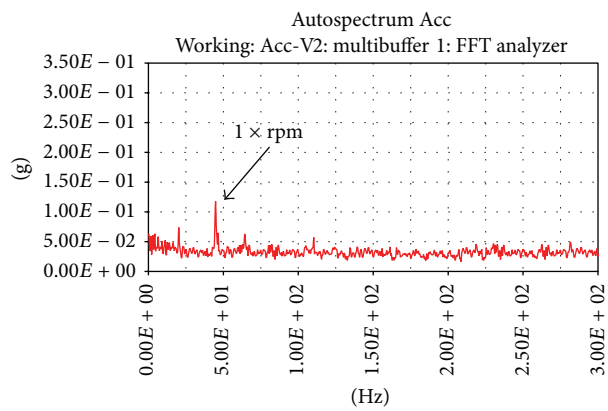

Figure 12: The rotor running supercritical at 2700 rpm (after balancing at 2nd set of correction planes of Case b).

correction masses. As is well-known, it is in general undecidable whether the set of critical modes are the only modes interacting with the flexible rotor unbalance. Therefore, it is important to consider the spillover from higher modes. Another equally important feature is related to the rotor's speed during measurements. Most of the modal balancing methods, in their mode-by-mode balancing procedure, adopt the policy of taking repeated measurements at or very close to the critical speeds. This is a stringent and sometimes impractical condition, as it is in general difficult to hold the rotor running steady at such transition speeds, where severe vibrations normally take place. This restrictive requirement is avoided by the developed method, which requires measurements at the running speed. This feature, not only avoids such operational difficulties, but also produces more representative measurements at the service speed, which is the primary concern. The main features of the developed scheme may be summarized as follows:

(i) Balancing supercritical rotors in the field, thus alleviating the cost of downtime and the cost of using a high-speed balancing facility.

(ii) No trial runs are needed.

(iii) Accounts for a good number of modes even above the highest critical speed.

(iv) Measurements are taken at the steady operating speed, thus avoiding the sever vibrations at critical speeds.

(v) The cost and effort are reduced drastically if several identical rotors are to be balanced, as the FEM model and the setup and preparation of both EMA and OMA will be the same for the identical rotors.

(vi) The simplicity of testing alternative sets of correction planes, which is very useful for supercritical flexible rotors of higher order.

While the above may look very much like an ideal scheme, there are some technical concerns that must be brought to the attention of the balancing expert. For instance, this technique requires the expertise of a modal analyst. The fidelity of the FEM model, which is common to all model-based techniques, is crucial to the balancing accuracy. The selection of planes may require testing other alternatives, especially when many critical speeds lie within the operating range. In general, the operating deflection shapes normally

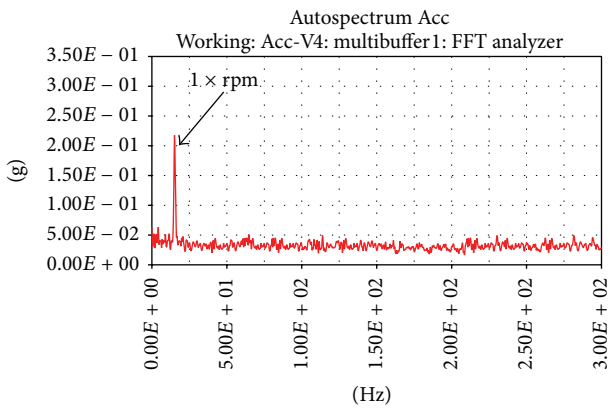

FIGURE 13: The rotor running supercritical at 900 rpm (after balancing at 2nd set of correction planes of Case b).

give good insight into the plane selection process. Moreover, the issue of sensitivity runs or trim balance may require the repetition of the entire procedure, which is also common to most balancing techniques.

As a direct extension to this work, one needs to test the developed technique in the field for actual rotors with relatively higher damping. Finally, two related issues may be posed for future research, namely, (a) the prediction of the number of significant modes associated with the flexible rotor imbalance and (b) finding the optimal set of correction planes for a supercritical flexible rotor.

Nomenclature

A: System coefficient matrix
C: Damping and Coriolis matrix
D: Modal submatrix
E: Modal submatrix
EMA: Experimental Modal Analysis
FEM: The Finite Element Method
H: Permutation of the identity matrix
K: Stiffness matrix
M: Mass matrix
m: Dimension of the modal transformation
N: Number of critical speeds in the operating range
ODS: Operational Deflection Shapes
OMA: Operational Modal Analysis
Q: Force vector
q: Nodal coordinate vector
U: Fourier transform of the modal vector

u: Modal coordinate vector
vec$(\cdot)$: Vector operator, as given in (6)
Acc-V2: Accelerometer output in vertical direction at second bearing
α: Imbalance
Φ: Modal matrix
ω: Frequency
$(\cdot)^{\dagger}$: Stands for the Moore-Penrose inverse.

Conflict of Interests

The authors declare that there is no conflict of interests regarding the publication of this paper.

Acknowledgments

This research work was funded by KACST Project no. AR-28–34. The authors acknowledge the support provided by King Abdulaziz City for Science & Technology (KACST) and King Fahd University of Petroleum & Minerals during this research.

References

[1] ISO Standard 1925, *Glossary of Terms Used in the Mechanical Balancing of Rotating Machinery*, 1981.

[2] ISO Standard 5343, *Recommendations For Criteria For Evaluating Flexible Rotors Balance*, 1983.

[3] ISO Standard 11342, *Methods and Criteria For the Mechanical Balancing of Flexible Rotors*, 1998.

[4] R. E. Bishop and A. G. Parkinson, "On the isolation of modes in the balancing of flexible shafts," *Proceedings of the Institute of Mechanical Engineers*, vol. 177, pp. 407–426, 1963.

[5] J. W. Lund and F. K. Orcutt, "Calculation and experiments on the unbalance response of a flexible rotor," *ASME Transactions, Journal of Manufacturing Science and Engineering*, vol. 89, no. 4, pp. 785–796, 1967.

[6] J. M. Tessarzik, R. H. Badgley, and W. J. Anderson, "Flexible rotor balancing by the exact point-speed influence coefficient method," *Journal of Engineering for Industry-Transactions of the ASME*, vol. 94, no. 1, pp. 148–158, 1972.

[7] R. E. Bishop and A. G. Parkinson, "On the use of balancing machines for flexible rotors," *ASME Transactions, Journal of Engineering for Industry*, vol. 94, no. 2, pp. 561–574, 1972.

[8] W. Kellenberger, "Should a flexible rotor be balanced in N or (N + 2) planes?" *ASME Transactions, Journal of Engineering for Industry*, vol. 94, no. 2, pp. 548–560, 1972.

[9] A. G. Parkinson, M. S. Darlow, and A. J. Smalley, "A theoretical introduction to the development of a unified approach to flexible rotor balancing," *Journal of Sound and Vibration*, vol. 68, no. 4, pp. 489–506, 1980.

[10] P. Gnielka, "Modal balancing of flexible rotors without test runs: an experimental investigation," *Journal of Sound and Vibration*, vol. 90, no. 2, pp. 157–172, 1983.

[11] P. G. Morton, "Modal balancing of flexible shafts without trial weights," *Proceedings of the Institution of Mechanical Engineers C, Mechanical Engineering Science*, vol. 199, no. 1, pp. 71–78, 1985.

[12] B. Xu, L. Qu, and R. Sun, "Optimization technique-based balancing of flexible rotors without test runs," *Journal of Sound and Vibration*, vol. 238, no. 5, pp. 877–892, 2000.

[13] J. K. Sinha, A. W. Lees, and M. I. Friswell, "Estimating unbalance and misalignment of a flexible rotating machine from a single run-down," *Journal of Sound and Vibration*, vol. 272, no. 3-5, pp. 967–989, 2004.

[14] G. Genta and F. De Bona, "Unbalance response of rotors: a modal approach with some extensions to damped natural systems," *Journal of Sound and Vibration*, vol. 140, no. 1, pp. 129–153, 1990.

[15] R. Zlatan, "Comprehensive analysis of a rotordynamic problem," in *Proceedings of the 3rd International Symposium on Stability Control of Rotating Machinery (ISCORMA-3)*, pp. 19–23, Cleveland, Ohio, USA, September 2005.

[16] S.-G. Tan and X.-X. Wang, "A theoretical introduction to low speed balancing of flexible rotors: unification and development of the modal balancing and influence coefficient techniques," *Journal of Sound and Vibration*, vol. 168, no. 3, pp. 385–394, 1993.

[17] L. Shi, "A modified balancing method for flexible rotors based on multi-sensor fusion," *Journal of Applied Sciences*, vol. 5, no. 3, pp. 465–469, 2005.

[18] Y. Kang, T.-W. Lin, Y.-J. Chang, Y.-P. Chang, and C.-C. Wang, "Optimal balancing of flexible rotors by minimizing the condition number of influence coefficients," *Mechanism and Machine Theory*, vol. 43, no. 7, pp. 891–908, 2008.

[19] G. N. D. S. Sudhakar and A. S. Sekhar, "Identification of unbalance in a rotor bearing system," *Journal of Sound and Vibration*, vol. 330, no. 10, pp. 2299–2313, 2011.

[20] X. Li, L. Zheng, and Z. Liu, "Balancing of flexible rotors without trial weights based on finite element modal analysis," *JVC/Journal of Vibration and Control*, vol. 19, no. 3, pp. 461–470, 2013.

[21] M. A. Mohiuddin and Y. A. Khulief, "Modal characteristics of rotors using a conical shaft finite element," *Computer Methods in Applied Mechanics and Engineering*, vol. 115, pp. 125–144, 1994.

[22] Y. A. Khulief and M. A. Mohiuddin, "On the dynamic analysis of rotors using modal reduction," *Finite Elements in Analysis and Design*, vol. 26, no. 1, pp. 41–55, 1997.

[23] M. A. Mohiuddin and Y. A. Khulief, "Coupled bending torsional vibration of rotors using finite element," *Journal of Sound and Vibration*, vol. 223, no. 2, pp. 297–316, 1999.

[24] J. W. Brewer, "Kronecker products and matrix calculus in system theory," *IEEE Transactions on Circuits and Systems*, vol. 25, no. 9, pp. 772–781, 1978.

[25] M. Khalil, S. Adhikari, and A. Sarkar, "Linear system identification using proper orthogonal decomposition," *Mechanical Systems and Signal Processing*, vol. 21, pp. 3123–3145, 2007.

[26] S. R. Ibrahim, "Dynamic modeling of structures from measured complex modes," *AIAA Journal*, vol. 21, no. 6, pp. 898–901, 1983.

[27] ISO 1940-1, "Mechanical vibrations: balance quality requirements of rigid rotors—part I," in *Determination of Permissible Residual Unbalance*, International Organization for Standardization, Geneva, Switzerland, 1986.

[28] ANSI/ASA S2.42 Revision 82, *American National Standard Procedures For Balancing Flexible Rotors*, 2004.

[29] ANSI/ASA S2.42 Revision 80, *Criteria For Evaluating Flexible Rotor Balance*, 2005.

[30] Y. A. Khulief and M. A. Mohiuddin, "Low-speed balancing for high-speed flexible rotors," KACST Technical Report AR-28-34, King Abdulaziz City for Science & Technology (KACST), Riyadh, Saudi Arabia, 2013.